Wannier Stark ladders in the optical absorption spectrum of a 'Hubbard exciton'

1989 J. Phys.: Condens. Matter 1 3325

(http://iopscience.iop.org/0953-8984/1/21/003)

J. Phys.: Condens. Matter 1 (1989) 3325–3336. Printed in the UK

Wannier Stark ladders in the optical absorption spectrum of a 'Hubbard exciton'

E R Chalbaud and J-P Gallinar
Departamento de Física, Universidad Simón Bolívar, Apartado 80659, Caracas 1080A, Venezuela

Received 24 August 1988

Abstract. A theory of absorption in a half-filled strong coupling extended Hubbard chain is applied to obtain the line shape of the optical absorption spectrum in the presence of a constant electric field E. As E is turned on, the zero-field spectrum breaks up into a complex asymmetrical structure of sharp peaks and gaps, associated to unevenly spaced Wannier Stark ladders of localised states of the electron–hole pair. The intensity of a Stark ladder peak becomes vanishingly small as the corresponding ladder rung number diverges. Two well defined absorption bands, arising from the parallel and the antiparallel alignment of the electric field E and exciton dipole moment, capture most of the intensity for a given E and sufficiently strong electron–hole mutual attraction V. For a given V, the lower-frequency (integrated) absorption intensity oscillates as a function of E, and then drops sharply to a constant value of half the total intensity as E further increases. The spin configuration of the Hubbard chain is found to have a significant influence upon the intensity of the absorption. Finally, some analytic results are presented when $E = 0$.

1. Introduction

Several authors have studied the motion of particles constrained to 'hop' on a lattice subject to various potential energy wells. Recently, Chalbaud *et al* (1986) analysed the quadratic or parabolic well. Prior to this, Gallinar and Mattis (1985) had considered the linear (electric) potential well, with special emphasis on hard-wall boundary conditions for the eigenfunctions of the well (see the review by Mattis 1986). Among other interesting results, unevenly spaced Wannier (Stark-ladder-like) eigenvalues were found for the spectrum of the well. Since its first prediction by Wannier (1959), the existence and nature of such ladder-like eigenvalues has remained a matter of considerable theoretical, as well as experimental, controversy (see, for example, Callaway 1974, Hart and Emin 1988). Thus, it may be worthwhile to take up similar studies again, but with a specific physical application in mind. In this paper a previously developed theory of optical absorption for a narrow half-filled Hubbard band chain (see Lyo and Gallinar 1977, Gallinar 1978), is re-examined and extended to include both the effect of a constant electric field E on the absorption spectrum of what we may call a 'Hubbard exciton', and that of a nearest-neighbour mutual electron–hole attraction V as well.

Because of the hard-wall-like relative hopping motion of its electron and hole, the interaction of the dipole moment of the 'Hubbard exciton' with the constant electric field E, gives rise to an effective linear potential well, and thus some of the predictions

0953-8984/89/213325 + 12 $02.50

of this Lyo and Gallinar (LG) absorption theory are related (where applicable) to those of the linear well considered by Gallinar and Mattis. In particular, it also predicts the existence of non-uniformly spaced (optical) Stark ladders. This mathematical parallel may be of greater interest than just a purely academic one. Indeed, Lyo and Gallinar's theory† has been used to interpret experimental features of the ($E = 0$) absorption spectra of some strongly correlated one-dimensional organic compounds such as potassium tetracyanoquinodimethane (TCNQ) (Yakushi *et al* 1979), or the infrared spectrum of dibenzotetraselenafulvalene-tetrafluoro-TCNQ (Jacobsen *et al* 1984). However, all of these previous sample measurements have been done *in the absence* of a constant E. Going one step further, we would like to conjecture (Fukuyama *et al* 1973) that for an appropriately large E, the optical absorption spectra of these insulating compounds (and other general alkali-TCNQs) might show experimental evidence of optical Stark ladders, such as are predicted by the theory considered in this paper for a narrow-band many-body insulator.

To this effect, it must be pointed out here that the optical experiments of Koss and Lambert (1972) in 'usual' insulators are generally‡ interpreted as indicative of the existence of the quantized Stark ladder. Analogous experiments for one-dimensional organic materials could then shed some valuable new light on this subject§.

Hence we certainly feel that the LG absorption theory is worth investigating on its own for $E \neq 0$, on account of its apparent suitability under zero-field conditions for appropriate one-dimensional organic insulators. Accordingly, some of our extensive numerical results concerning this interesting matter are presented below, and further analytical findings are also given for the zero-field case.

2. Formalism

We consider the extended Hubbard (1978) Hamiltonian, with a constant E superimposed along the chain direction, as

$$H = -t \sum_{j,\sigma,\delta=\pm 1} c^{+}_{j+\delta,\sigma} c_{j,\sigma} + U \sum_{j} n_{j\uparrow} n_{j\downarrow} + V \sum_{j} n_j n_{j+1} + \alpha \sum_{j} j n_j \qquad (1)$$

where t is the transfer integral, U is the on-site and V the nearest-neighbour Coulomb interaction. $c^{+}_{j,\sigma}(c_{j,\sigma})$ creates (destroys) an electron of spin σ at site j, $n_{j,\sigma} = c^{+}_{j,\sigma} c_{j,\sigma}$ is the occupation number; $n_j = \Sigma_\sigma n_{j,\sigma}$, and $\alpha \equiv |e|Ea$, where e is the electronic charge and a is the lattice constant. The absorption spectrum $\sigma(\omega)$ is given by the real part of the complex conductivity. By a simple extension of the LG theory (see, for example, Gallinar 1979a), one can obtain $\sigma(\omega)$ in terms of a continued fraction expression as

$$\sigma(\omega) = \frac{N\pi e^2 a^2 t^2 p}{U\Omega} \int_0^1 \mathrm{d}x\, Q(x, \beta)\rho_0(\omega; x) + [\alpha \leftrightarrow -\alpha] \qquad (2)$$

where N, Ω, p are the number of lattice sites, the volume of the sample, and the probability of initial electron–hole pair creation ('Hubbard exciton'), respectively. We

† Suitably extended by the inclusion of a nearest-neighbour electron–hole attraction V.

‡ Unfortunately, no universal agreement exists on this interpretation (see Krieger and Iafrate 1986).

§ To the best of our knowledge such experiments have yet to be done.

have

$$\rho_0(\omega; x) = \frac{1}{\pi} \operatorname{Im} \left(z - \alpha + V - \frac{(2tx)^2}{z - 2\alpha -} \frac{(2tx)^2}{z - 3\alpha -} \cdots \right)^{-1} \tag{3}$$

with $z \equiv \omega - U - i\delta$. The second (bracketed) term in (2) corresponds to the parallel alignment of the exciton dipole moment with E. It is obtained from the first (or anti-parallel) term by the substitution $\alpha \leftrightarrow -\alpha$. $\rho_0(\omega; x)$ as given by (3) may be thought of as a local 'density of states' for the electron and hole when separated by distance a. Finally, the weight function $Q(x, \beta)$ is given by

$$Q(x, \beta) = (2 \cos \beta)/[\pi(1 - x^2 \sin^2\beta)(1 - x^2)^{1/2}] \tag{4}$$

with $p \equiv \tan^2(\beta/2)$, and $0 \leq \beta \leq \pi/2$. For $p = 1$ we have an antiferromagnetic (AF) spin arrangement in the Hubbard chain, and

$$Q(x, \pi/2) = \delta(x - 1). \tag{4'}$$

For $p = 1/2$ and $p = 0$, the spin arrangement is random (R) and ferromagnetic (F), respectively.

We have evaluated the continued fraction in (3) analytically in terms of Bessel functions $J_\nu(y)$ of the first kind. After some manipulations, we find

$$\rho_0(\omega; x) = \frac{1}{\pi} \operatorname{Im} \left(\frac{J_{1 - z/\alpha}(y)}{VJ_{1 - z/\alpha}(y) - 2txJ_{-z/\alpha}(y)} \right) \tag{5}$$

where $y \equiv 4tx/\alpha$. From (2), (3), and (5), we then write $\sigma(\omega)$ in the form

$$\frac{\sigma(\omega)}{K} = \sum_k \int_0^1 \mathrm{d}x \, Q(x, \beta) R_k(x) \delta\{\omega - U - \omega_k(x)\} + [\alpha \leftrightarrow -\alpha] \tag{6}$$

with $K \equiv N\pi e^2 a^2 t^2 p / U\Omega$, and where the summation over k extends to all the simple roots $\omega_k(x)$ of the equation

$$VJ_{1 - \omega_k/\alpha}(y) = (2tx)J_{-\omega_k/\alpha}(y) \tag{7}$$

i.e., to all the poles of the continued fraction in (5) (or in (3)), with corresponding residues $R_k(x)$. For $V = 0$, equation (7) reduces to the condition

$$J_{-\omega_k/\alpha}(y) = 0. \tag{8}$$

An equation formally equivalent to (8) was previously considered by Gallinar and Mattis (1985) in their study of the linear potential well problem. By itself it yields a non-uniformly spaced (optical) Stark ladder spectrum ω_k. It must be noted that (8) has also been considered, at various times, by other authors (Fukuyama *et al* 1973, for example) in rather diverse contexts. Proceeding further, the integration over x in (6) finally yields

$$\frac{\sigma(\omega)}{K} = \sum_{k,i} \frac{Q(x_i, \beta) R_k(x_i)}{|\mathrm{d}\omega_k/\mathrm{d}x|_{x = x_i}} + [\alpha \leftrightarrow -\alpha] \tag{9}$$

with the x_i being those simple roots of the equation $\omega - U - \omega_k(x_i) = 0$ that satisfy $0 \leq x_i \leq 1$. We have evaluated (6) and (9) numerically for different values of the parameters α, V and p. Some of our results in this rich parameter space are discussed briefly below.

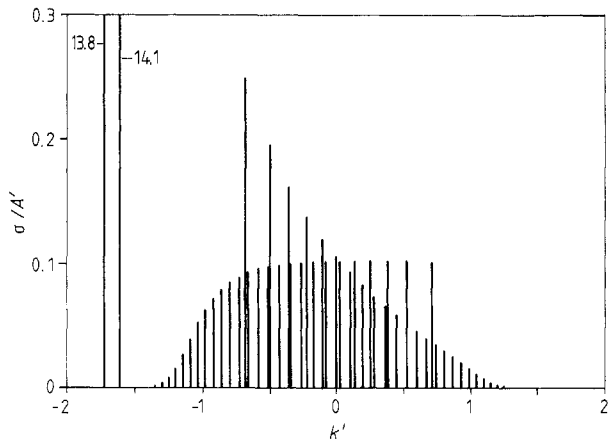

Figure 1. Plot of $\sigma(\omega)/A'$ versus $k' \equiv (\omega - U)/4t$, with $A' \equiv K/2t$. For display purposes the δ-function peaks in (10) have been given a small width $\delta k' = (10\pi)^{-1}$. The total area under the plotted curve is normalised to one. $v = 3, p = 1$ and $\alpha/t = 0.2$.

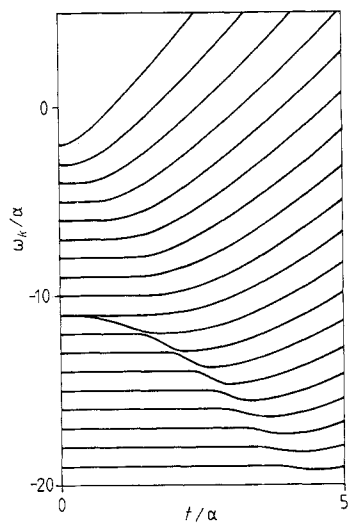

Figure 2. Plot of $\omega_k(1)/\alpha$ versus t/α for $V/\alpha = 10$ and a parallel dipole moment orientation *only*; $k = 1, 2, \ldots, 19$. Because of the electron–hole attraction $(-V)$, the $(t = 0)$ state with $\omega_1/\alpha = -1$, has moved down to (-11), where it induces a characteristic 'repulsion' of nearby ladder levels when $t \neq 0$.

3. Results and discussion

In figure 1, we show the spectrum obtained for $p = 1$, $(V/2t) \equiv v = 3$ and $\alpha/t = 0.2$. With $t \simeq 0.1$ eV this corresponds to a field E on the order of 10^5 V cm^{-1}. Using the property (4'), for this $(p = 1)$ AF case we can write (6) in the form

$$\sigma(\omega)/K = \sum_k R_k(1)\delta[\omega - U - \omega_k(1)] + [\alpha \leftrightarrow -\alpha]. \tag{10}$$

Thus, as shown in the figure 1, the optical spectrum given by (10) consists of two (semi-) infinite series of discrete δ-function peaks which partially interlace each other. One series, or Wannier–Stark ladder, exists for each orientation of the exciton dipole moment. Each δ-peak is centred at an optical Stark ladder frequency $U + \omega_k(1)$, with the non-uniform spacing of the rungs of each ladder clearly visible in figure 1. With increasing ladder rung number $(k \to \infty)$, the intensity associated with a corresponding peak becomes vanishingly small, and, as can be seen, each Stark ladder is ultimately characterised by *evenly* spaced rungs with $\omega_k(1) \to \pm k\alpha$, in the limit $k \to \infty$. The origin of this last behaviour can be qualitatively understood from figure 2, where a $\omega_k(1)$ spectrum (for the parallel dipole moment) is displayed as a function of t/α†. When $k \to \infty$, a general feature of such spectra is that the eigenvalues $\omega_k(1) \simeq \pm k\alpha$ ultimately become flat or t-independent, and are thus evenly spaced.

Returning to figure 1, to the left two intense peaks can be seen, with heights of 13.8 and 14.1. The former (latter) corresponds to parallel (antiparallel) alignment of E and

† Note from equation (7), that $\omega_k(x)$ depends upon x only through the combination (tx).

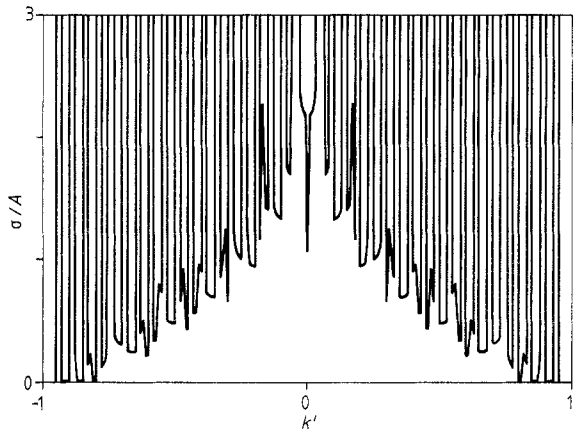

Figure 3. Plot of $\sigma(\omega)/A$ versus k', with $p = v = 0$, and same electric field as in figure 1; $A \equiv K/\pi t$. Only the region $|k'| < 1$ is shown here. Notice the incipient appearance of gaps in the spectrum for $|k'| \geq 0.8$, wherein $\sigma(\omega)$ actually vanishes.

the exciton dipole moment. Between the two they capture most (here 89%) of the total absorption intensity (i.e., the area under the curve). In general, for strong enough $v > 1$ two such peaks will be approximately located at

$$k'_{1,2} \simeq -[(v + v^{-1})/2] \pm \alpha/4t \tag{11}$$

and can be thought of as 'excitonic absorption' of the electron and hole when they are nearest neighbours. Two such peaks are discussed below (see figure 6).

We turn now to the case $p \neq 1$. In figure 3 we show the spectrum for $p = v = 0$, obtained from equation (9) (with same $\alpha/t = 0.2$ as in figure 1). For $p < 1$, the δ-function peaks of the AF ($p = 1$) case are now smeared out into sharp divergences. If $V = 0$, these arise in equation (9) from the inverse-square-root divergence of the function $Q(x_i, \beta)$ when $x_i(\omega) \to 1$. If $V \neq 0$, it can be proved that additional sharp structure is also obtained from the vanishing of the derivative $(\mathrm{d}\omega_k/\mathrm{d}x)_{x=x_i}$. Note also the symmetry of σ about $k' = 0$. If $V = 0$, it can be seen from (2) and (3) that the spectrum is symmetrical, i.e., $\sigma(k') = \sigma(-k')$, *always*. Finally, we notice how the 'bottom profile' of $\sigma(\omega)$ in figure 3 closely 'resembles' a corresponding zero-field ($\alpha = 0$) spectrum with $p = v = 0$ previously obtained by Lyo and Gallinar (1977). To enable comparison with such previous results, the total absorption intensity area in figure 3 has therefore been set at $\pi/2$. In figure 4 we have doubled the electric field of figure 3, and have smoothed out the sharp divergences of its spectrum by a 'coarse-graining' procedure. This is done numerically in equation (6) by approximating $\sigma(\omega)$ with the expression

$$\frac{1}{\Delta\omega}\int_{\omega}^{\omega+\Delta\omega} \sigma(\omega)\,\mathrm{d}\omega$$

where a suitably small 'grain' $\Delta\omega$ is chosen. By comparing figures 3 and 4, we see that the coarse-graining procedure visually enhances the significant absorption profile of $\sigma(\omega)$ which was previously 'obscured' by the divergences present in figure 3. Up to the numerical accuracy involved, the graining procedure also preserves the total absorption intensity area under $\sigma(\omega)$.

Figures 5, 6 and 7 all refer to a $p = \frac{1}{2}$, or random spin arrangement in the Hubbard chain. In figure 5 we have the asymmetry typical of the spectra with $V \neq 0$. Because of the negative $(-V)$ energy of the electron and hole mutual attraction, the absorption intensity tends to be stronger for $k' < 0$, i.e., the $\sigma(\omega)$ curve is shifted to the left of the

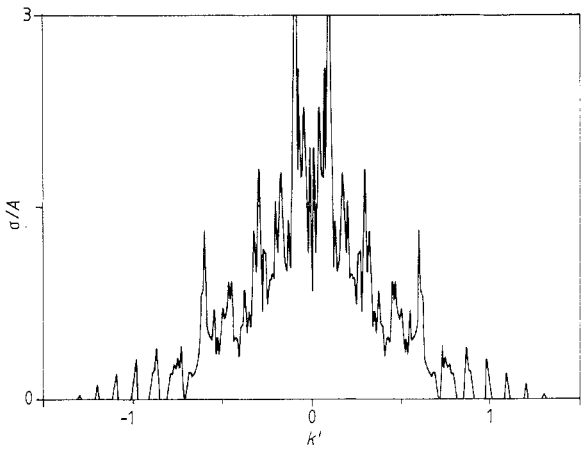

Figure 4. Plot of coarse-grained $\sigma(\omega)/A$ versus k'. The chosen graining is given by $\Delta k' \equiv \Delta\omega/4t = 10^{-2}$. Because of stronger field E, the first gap appears here for smaller $|k'| = 0.7$, than in figure 3. The vanishingly small absorption peaks for $|k'| \gg 1$ are a striking example of the (equally spaced) optical Stark ladder. $v = 0$, $p = 0$ and $\alpha/t = 0.4$.

figure. Indeed, reading from figure 8, we see that the $k' < 0$ integrated absorption intensity of this (figure 5) spectrum represents about 85% of its total absorption intensity. The spectrum of figure 5 should be contrasted with a ($v = 1.001$) corresponding zero-field ($\alpha = 0$) spectrum in figure 7. The strikingly complex structure created by the electric field is truly quite amazing.

In figure 6, we see the two strong δ-peaks of figure 1 that have now broadened into the respective absorption bands typical of $p \neq 1$ in equation (6). The two bands partially

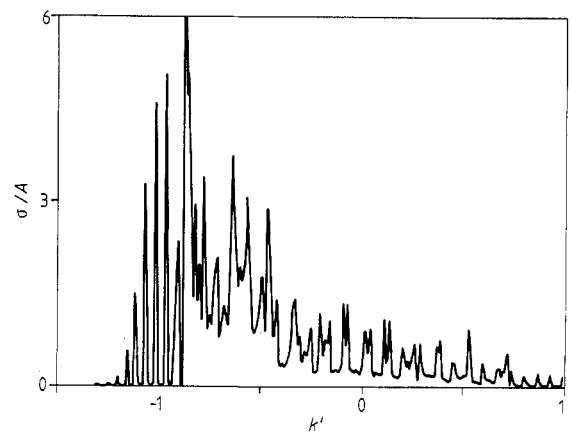

Figure 5. Plot of coarse-grained $\sigma(\omega)/A$ versus k', with same graining $\Delta k'$ as in figure 4. Only the region $k' \leq 1$ is shown here. For $k' > 1$ the spectrum becomes extremely small. $v = 1$, $p = \frac{1}{2}$ and $\alpha/t = 0.2$.

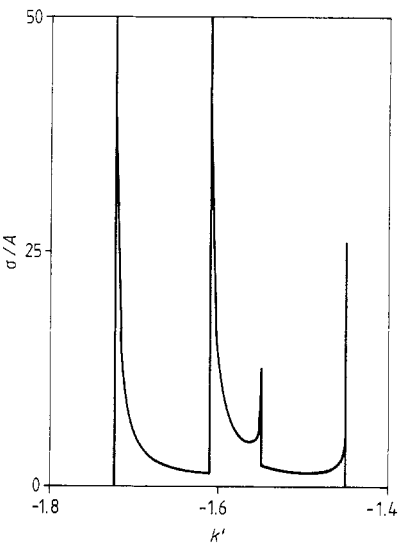

Figure 6. Close-up plot of coarse-grained $\sigma(\omega)/A$ versus k' in the restricted region $-1.8 \leq k' \leq -1.4$. The (smaller) graining is set at $\Delta k' = 2.5 \times 10^{-4}$ and no evidence of 'wiggly' structure is present on this scale. $v = 3$, $p = \frac{1}{2}$ and $\alpha/t = 0.2$.

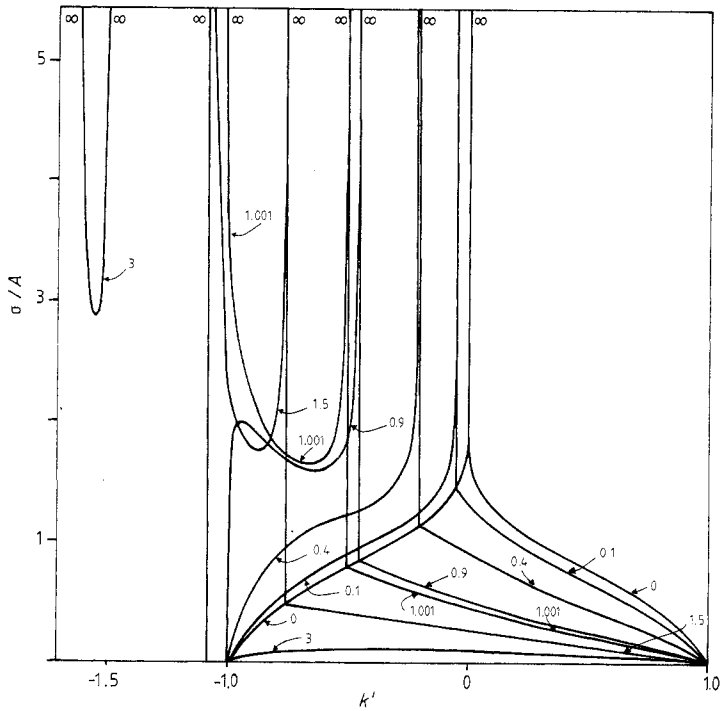

Figure 7. Plot of a zero-field $\sigma(\omega)/A$ versus k', for different values of v indicated by the small arrows. For $k' \geq 1$ the spectrum vanishes identically. $p = \frac{1}{2}$ and $\alpha/t = 0$.

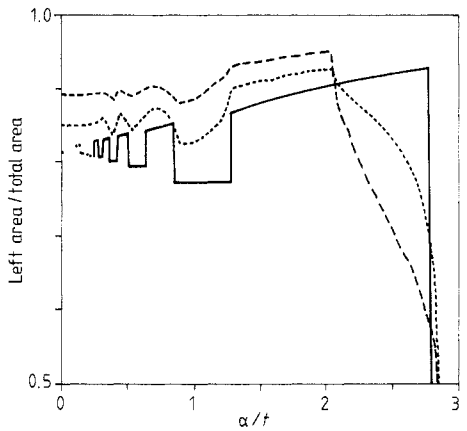

Figure 8. Plot of (relative) integrated absorption intensity in the lower-frequency ($k' \leq 0$) region, versus α/t. For visual convenience, only a few points are shown when $\alpha/t \leq 0.25$ in the $p = 1$ curve. If $\alpha/t \geq 2.8$, the relative intensity is constant and equal to $\frac{1}{2}$, but the spectrum can be asymmetrical. $v = 1$; ---, $p = 0$; ·····, $p = \frac{1}{2}$; ——, $p = 1$.

overlap, and according to equation (11) their respective lower edges are given by $k_1' = -1.61$, and $k_2' = -1.72$. The total intensity of their absorption is slightly greater here (91%) than in figure 1 (89%). This is an example of a general trend: as p decreases, the intensity of the two peaks increases. We have discovered many other such interesting trends; they will be reported upon elsewhere. Figure 6 should also be compared with the corresponding zero-field ($v = 3$) spectrum in figure 7. As can be seen, when $E = 0$ the two 'excitonic absorption' bands then overlap completely into a single strong absorption peak.

Finally, in figure 8 the relative intensity of the lower-frequency ($\omega \leqslant U$) absorption is plotted (for $v = 1$) as a function of electric field. Because the weight function $Q(x, \beta)$ satisfies the (β-independent) condition

$$\int_0^1 \mathrm{d}x\, Q(x, \beta) = 1$$

$\sigma(\omega)$ satisfies the sum rule

$$\int \mathrm{d}\omega\, \sigma(\omega) = 2K \tag{12}$$

(note that one has $\Sigma_k R_k(x) = 1$ in equation (6)). Thus, the total area under $\sigma(\omega)$ is field-independent. Figure 8 then exhibits how the integrated absorption intensity for $\omega \leqslant U$ (given by the 'left area') 'oscillates' with growing amplitude as a function of increasing applied field. This oscillatory behaviour persists up to a certain field (which increases with v, but is roughly independent of p), above which the ($\omega \leqslant U$) intensity is constantly half the total. For the $v = 1$ case shown in this figure 8 a strong field of about 10^6 V cm^{-1} is needed before the sharp drop is attained. Note also how the abrupt oscillations present for $p = 1$ become smoother for decreasing p. The oscillations occur every time the Stark ladder frequency curves $\omega_k(1)$ (such as those in figure 2) intersect a straight horizontal line drawn through the point (0, 0) of figure 2. When the intersection occurs with a curve $\omega_k(1)$ for the parallel (antiparallel) dipole moment alignment, the left area goes down (up). As a consequence, for $\alpha/t \to 0$ we get an infinite number of oscillations with ever-decreasing amplitude and width. Since they cannot be fully illustrated on this (or any other) scale, we have plotted a few points in the region $\alpha/t \leqslant 0.25$. Another interesting feature of figure 8 is the ordering of the intensities with respect to p. The intensities increase with decreasing p for field values up to $\alpha/t \simeq 2$, at which point the order is reversed. Finally, we stress that an increasing electron–hole attraction leaks intensity from the $k' > 0$ region into the region $k' < 0$, and that for strong enough v the two excitonic absorption peaks (or bands) will both lie in the $k' < 0$ region, thus contributing to the left area intensity plotted in this figure.

4. Zero-field spectrum

Having numerically studied in some detail the electric field effects, we turn now to a brief analytical digression concerning the field-free spectrum. By itself, it serves both as a point of comparison and of illustrative contrast to the spectra obtained here. Both Lyo (1978) and Gallinar (1979b) have partially considered it previously, but here we present a more complete analytical solution in terms of elliptical integrals. This may then give the reader a somewhat more thorough example of the application of our formalism.

If we set $\alpha = 0$ in equation (3), the resulting continued fraction can be evaluated easily in terms of elementary functions. After a straightforward analysis we find from (2), (3) and (9) that $\sigma(\omega) = \sigma_1(\omega) + \sigma_2(\omega)$, where

$$\frac{\sigma_1(\omega)}{K} = \frac{1}{\pi}\int_0^1 \mathrm{d}x\, Q(x, \beta)\, \frac{[(4tx)^2 - (\omega - U)^2]^{1/2}}{V(\omega - U + V) + (2tx)^2} \tag{13}$$

arises from a 'continuous' density of states $\rho_0(\omega; x)$ in (3), and can be evaluated in terms of elliptical integrals (see Appendix 1), while

$$\frac{\sigma_2(\omega)}{K} = \frac{2Q(x_1, \beta)R_1(x_1)}{|\mathrm{d}\omega_1/\mathrm{d}x|_{x=x_1}} \tag{14}$$

arises from a single pole $\omega_1(x)$ in (3). In (14) we have

$$R_1(x) = [1 - (2tx)^2/V^2]u[1 - (2tx/V)]$$

where $u[1 - (2tx/V)]$ is the unit step function; and $|\mathrm{d}\omega_1/\mathrm{d}x| = 8t^2x/V$, since

$$\omega_1(x) = -V - [(2tx)^2/V]. \tag{14'}$$

The point $x_1(\omega)$ is given by the roots of the equation $\omega_1(x_1) = \omega - U$, such that $0 \leq x_1(\omega) \leq 1$. Thus,

$$x_1(\omega) = \{[-V(\omega - U + V)]/4t^2\}^{1/2} \equiv [-v(2k' + v)]^{1/2} \tag{15}$$

and if $0 \leq x_1(\omega) \leq 1$, then k' must satisfy the inequalities

$$-(v + v^{-1})/2 \leq k' \leq -v/2 \tag{15'}$$

for $\sigma_2(\omega)$ *not* to vanish. Upon final substitutions in (14), we obtain (with $A \equiv K/\pi t$) that

$$\sigma_2(\omega) = \frac{2A(v - |k'|)u(v - |k'|)u(1 - x_1)\cos\beta}{x_1(1 - x_1^2)^{1/2}(1 - x_1^2\sin^2\beta)}. \tag{16}$$

In figure 7 we have plotted $\sigma_1(\omega) + \sigma_2(\omega)$ for $p = \frac{1}{2}$ and increasing values of v, up to $v = 3$. As v is turned on, the $k' = 0$ logarithmic singularity of $\sigma(\omega)$ present for $v = 0$, changes into a stronger inverse-square-root singularity which moves to the left point $k' = -v/2$. This singularity in $\sigma(\omega)$ arises from the vanishing of $x_1(\omega)$ in (16), i.e., of $(\mathrm{d}\omega_1/\mathrm{d}x)_{x=x_1}$ in (14). Curiously, if $k' \to -v/2$ from above, then $\sigma(\omega)$ tends to the 'unperturbed' value of the $(v = 0)$ spectrum at the point $k' = -v/2$. As v continues increasing up to $v = 1$, more intensity is progressively leaked into the region $-1 \leq k' \leq 0$, the spectrum becoming very asymmetrical. This continues until the value $v = 1$ is reached, and a second inverse-square-root singularity appears in $\sigma_2(\omega)$ at the point $k' = -1$ (i.e., for $x_1(\omega) \to 1$). This effect can be clearly seen in figure 7, where the spectra for $v = 0.9$ and $v = 1.001$ can be contrasted. For $v > 2$, both singularities finally leave the unperturbed spectrum region, and a strong 'excitonic absorption' peak emerges to the left of the $(v = 0)$ spectrum. This excitonic peak has its lower edge at

$$\omega = U + \omega_1(1) = U - V - (4t^2/V) \tag{17}$$

according to (14') and (15'). In Appendix 2 we show how this edge position can also be extracted, in the zero-field limit ($\alpha \to 0$), from equation (7) defining the Wannier–Stark ladder frequencies.

5. Summary

Although the optical Stark-ladder-like spectra found in this work are extremely complex, and defy detailed description in any direct analytical manner, it is clear from the above that the simpler field-free ($\alpha = 0$) case serves as a useful reference point for interpreting them. As such we have presented it here, and proceed now to summarise our main results when $E \neq 0$.

For the antiferromagnetic ($p = 1$) ground state of a strong-coupling extended Hubbard chain, we have found that the electric field drastically changes the field-free spec-

trum into two semi-infinite optical Stark ladders. These ladders partially interlace with each other; their rungs become equally spaced only above and below the field-free continuous spectrum. For the random ($p = \frac{1}{2}$) and ferromagnetic ($p = 0$) spin arrangements, the ladders' rungs broaden into a sharp but continuous (complex) structure of peaks and gaps. An interesting field-dependent oscillatory structure has also been found in the partially integrated absorption intensity (as opposed to the total one, which is field-independent according to the sum rule in (12)). This oscillatory structure is a clear manifestation of the optical Stark ladders previously found. By raising the temperature above the Néel point $\sim t^2/U$, we obtain the random spin arrangement and a smoothing of the intensity oscillations. Finally, the application of a strong magnetic field inducing a ferromagnetic spin arrangement, also results in a further smoothing of these oscillations.

Appendix 1

We show that $\sigma_1(\omega)$ in (13) can be expressed in terms of the complete elliptical integrals. In fact, we expand in partial fractions the rational function of x that appears as part of the integrand in (13). Then we find for (13) the expression

$$\sigma_1(\omega) = \frac{2A(\cos\beta)[(\gamma^2 - 1)\Pi(\gamma^2, k) - (\delta^2 - 1)\Pi(\delta^2, k)]}{\pi[1 + v(2k' + v)\sin^2\beta]} \tag{A1.1}$$

where $\Pi(\gamma^2, k)$ and $\Pi(\delta^2, k)$ are complete elliptical integrals of the third kind (Byrd and Friedman 1954), with parameters

$$\gamma^2 \equiv \frac{k^2}{1 + v(2k' + v)} \qquad \delta^2 \equiv -k^2\tan^2\beta \qquad k \equiv (1 - k'^2)^{1/2}.$$

Since $\delta^2 \leqslant 0$, the integral $\Pi(\delta^2, k)$ is always in a 'circular' case and, thus, can be evaluated in terms of Heuman's lambda function $\Lambda_0(\beta, k)$ (Byrd and Friedman 1954). After a series of transformations, there results

$$\sigma_1(\omega) = \frac{2A(\cos\beta)u(1 - |k'|)}{\pi[1 + v(2k' + v)\sin^2\beta]}\{(\gamma^2 - 1)\Pi(\gamma^2, k) + (1 - k'^2\sin^2\beta)K(k) + (\pi/2)(\tan\beta)(1 - k'^2\sin^2\beta)^{1/2}\Lambda_0(\beta, k)\} \tag{A1.2}$$

where $u(1 - |k'|)$ is the unit step function, and $K(k)$ is the complete elliptical integral of the first kind.

Concerning the integral $\Pi(\gamma^2, k)$ in (A1.2), we must distinguish two different cases. If $2k' + v \leqslant 0$, then $k^2 \leqslant \gamma^2 \leqslant 1$, and the integral is also in a circular case. Expressing it in terms of Heuman's lambda function, we obtain that

$$(\gamma^2 - 1)\Pi(\gamma^2, k) = \frac{-\pi|\cot\xi|\Lambda_0(\xi, k)}{2(1 - v|2k' + v|)^{1/2}}$$

in (A1.2); where the angle ξ is defined through $|k'|\sin\xi \equiv (v|2k' + v|)^{1/2}$.

On the other hand, if $2k' + v \geqslant 0$, then $0 \leqslant \gamma^2 \leqslant k^2$, and the integral $\Pi(\gamma^2, k)$ is in a 'hyperbolic' case. It can then be evaluated in terms of Jacobi's zeta function $Z(\theta, k)$, leading finally to

$$\sigma_1(\omega) = \frac{2A(\cos\beta)u(1-|k'|)}{\pi[1+v(2k'+v)\sin^2\beta]}\left\{K(k)\left[\frac{Z(\theta,k)}{\sin\theta[1+v(2k'+v)]^{1/2}} - k'^2\sin^2\beta\right]\right.$$
$$\left. + (\pi/2)(\tan\beta)[1-k'^2\sin^2\beta]^{1/2}\Lambda_0(\beta,k)\right\}$$

where the angle θ is defined by $k'\tan\theta = [v(2k'+v)]^{1/2}$.

Appendix 2

In this Appendix we show how to obtain equation (17) from equation (7), in the limit $\alpha \to 0$.

With $x = 1$, we rewrite equation (7) in the form

$$J_\nu(\nu\,\mathrm{sech}\,\lambda) = (V/2t)J_{\nu'}(\nu'\,\mathrm{sech}\,\mu) \tag{A2.1}$$

where

$$\nu \equiv -[\omega_1(1)/\alpha] > 0 \qquad \nu' \equiv \nu + 1 \qquad \cosh\lambda \equiv [-\omega_1(1)/4t] \geqslant 1$$

and $\cosh\mu \equiv \cosh\lambda + \alpha/4t$. If $\alpha \to 0$, then we have $\nu \to \infty$, and we can use the asymptotic expansions for large order of the Bessel functions in (A2.1). Equation (A2.1) then becomes (Abramowitz and Stegun 1965) with λ and μ both positive

$$\frac{\exp[\nu(\tanh\lambda - \lambda)]}{(\nu\tanh\lambda)^{1/2}} = \left(\frac{V}{2t}\right)\frac{\exp[\nu'(\tanh\mu - \mu)]}{(\nu'\tanh\mu)^{1/2}} \tag{A2.2}$$

and, since $\nu' \to \nu$; $\mu \to \lambda$, we obtain from (A2.2)

$$V/2t = \exp[\nu(\tanh\lambda - \lambda - \tanh\mu + \mu)]$$
$$= \exp[(4t/\alpha)(\sinh\lambda - \lambda\cosh\lambda - \sinh\mu + \mu\cosh\mu)]$$
$$= \exp[(4t/\alpha)\mu(\cosh\mu - \cosh\lambda)] = \exp\lambda. \tag{A2.3}$$

Using now the logarithmic representation for $\cosh^{-1}[-\omega_1(1)/4t]$ in $\exp\lambda$, we finally get from (A2.3) that

$$\frac{V}{2t} = \frac{-\omega_1(1)}{4t} + \left[\left(\frac{\omega_1(1)}{4t}\right)^2 - 1\right]^{1/2} \qquad \text{or} \qquad \omega_1(1) = -V - (4t^2/V) \qquad \text{QED.}$$

Somewhat similar procedures enable one to show from (7) that for $|\omega_k(1)| \leqslant 4t$ and $\alpha \to 0$, there is, additionally, a dense accumulation of frequency roots that ultimately give rise to $\sigma_1(\omega)$ in (13).

Acknowledgments

The support of this research by the Consejo Nacional de Investigaciones Científicas y Tecnológicas (CONICIT) under Grant No. S1-1207 is gratefully acknowledged. We are indebted to Professor D C Mattis for bringing Fukuyama *et al* (1973) to our attention, and for a preprint of Hart and Emin (1988), too.

References

Abramowitz M and Stegun I A 1965 *Handbook of Mathematical Functions* (New York: Dover)
Byrd P F and Friedman M D 1954 *Handbook of Elliptical Integrals for Engineers and Physicists* (Berlin: Springer)
Callaway J 1974 *Quantum Theory of the Solid State* (New York: Academic)
Chalbaud E, Gallinar J-P and Mata G 1986 *J. Phys. A: Math. Gen.* **19** L385
Fukuyama H, Bari R and Fogedby H 1973 *Phys. Rev.* B **8** 5579
Gallinar J-P 1978 *Phys. Rev.* B **17** 807
—— 1979a *J. Phys. C: Solid State Phys.* **12** L335
—— 1979b *Phys. Lett.* **70A** 353
Gallinar J-P and Mattis D C 1985 *J. Phys. A: Math. Gen.* **18** 2583
Hart C F and Emin D 1988 *Phys. Rev.* B **37** 6100
Hubbard J 1978 *Phys. Rev.* B **17** 494
Jacobsen C S, Johannsen Ib and Bechgaard K 1984 *Phys. Rev. Lett.* **53** 194
Koss R W and Lambert L M 1972 *Phys. Rev.* B **5** 1479
Krieger J B and Iafrate G J 1986 *Phys. Rev.* B **33** 5494
Lyo S K 1978 *Phys. Rev.* B **18** 1854
Lyo S K and Gallinar J-P 1977 *J. Phys. C: Solid State Phys.* **10** 1693
Mattis D C 1986 *Rev. Mod. Phys.* **58** 361
Wannier G H 1959 *Elements of Solid State Theory* (Cambridge: Cambridge University Press)
Yakushi K, Kusaka T and Kuroda H 1979 *Chem. Phys. Lett.* **68** 139